Armenian Journal of Physics, 2021, vol. 14, issue 2, pp. 117-127

About memristive effects in M-Ba(Sr)TiO_3-M thin film structure

V.V. Buniatyan*, H.R. Dashtoyan, L.G. Rustamyan

National Polytechnic University of Armenia (NPUA), 105 Teryan St, 0009, Yerevan, Armenia

*E-mail: vbuniat@seua.am, vbuniat@yahoo.com

Received 5 June 2021

Abstract. Trapping/detrapping characteristics of thin film metal-ferroelectric-metal (m-f-m, Pt-$Ba_xSr_{1-x}TiO_3$-Pt) structure is considered assuming that the ferroelectric is in paraelectric phase and high concentration of oxygen vacancies (OV) in the interfacial regions of metal-ferroelectric contacts. It is assumed that these vacancies create electron trap levels in the band gap of the ferroelectric. At high electric fields (or at high temperatures) the oxygen vacancies are ionized due to detrapping of electrons via Pool-Frenkel emission which leads to change essentially the trap levels occupation function, $f_t(E,t)$, and hence created a new non-compensated oxygen vacancies. These newly created charged vacancies, in turn, can change internal state, as well as m-f interfacial potentials, and thus may alter all processes of its based memristors. The nonlinear dependence of permittivity on applied electric field is taken into account too. Based on these assumptions analytical expression for the DC bias dependent traps level occupation function, $f_t(E,t)$, its time dependence and ferroelectric material fundamental parameters dependencies are derived for the first time.

https://doi.org/10.52853/18291171-2021.14.2-117

Keywords: ferroelectric, oxygen vacancy, trapping/detrapping level, Pool-Frenkel emission

1. Introduction

Nonvolatile resistance switching (RS) is a seemingly universal phenomenon exhibited by metal-oxide-metal thin-film capacitor structures, particularly metal-ferroelectric-metal structures [1-8]. Ferroelectric based ReRAM is one of the most promising candidates for next negation of non-volatile memory due to characteristics such as its simple structure, as high-density, high scalability, high switching speed, low cost, fast write and read access, low energy operation, and high performance with respect to endurance (write cyclability) and retention (non volatility) [9-17]. Its compatibility with the current CMOS technology ensures a promising scaling down prospective. In the non-volatile memory application areas, the problems of retention, endurance, switching speed, leakage mechanisms, yield, and noise immunity are at the infant research stage. In spite of all these constraints, the novelty of memristor to combine computing, logic and memory on a single platform is a driving force behind the research and industry interest.

Many suggested mechanisms have been put forward to explain the causes of resistance switching [3, 5, 8-17] which can be split into two groups: ionic (involve the migration of oxygen vacancies) and thermal (where the application of an electric field and flowing current heats the material and changes its structure) [18-20]. Based on their “scale” those RS mechanisms can be classify also as: carrier trapping/detrapping (electronic scale), migration of point defect (atomic scale), metal-insulator ransition (apparent change of the atomic structure), thermochemical reaction (apparent change of the microstructure), and complex mechanism. The three main classes are based on an electrochemical metallization mechanism, a valence change mechanism, and a thermochemical mechanism, respectively. The changes of the resistance due to various mechanisms

are actually caused by the evolution of these defected structures triggered by the electric/thermal effects, a typical structure-property relation in materials science.

Among these mechanisms there are many analyses indicating the importance of both trap-controlled space-charge-limited current and Poole–Frenkel effect in resistance switching [20, 21].

Vacancy motion was responsible for switching in $SrTiO_3$, $La_{0,7}Ca_{0,3}MnO_3$, as well as in Ca doped $BiFeO_3$ grown on $SrTiO_3$ [21-25]. The results reiterated the importance of point defects, mainly oxygen vacancies and their movements in controlling electrical switching behavior of memristors. This concept then has been developed in [12] as the first complete quantitative model for bipolar switching in oxides based vacancy drift/diffusion and showed that this model is equivalent to the memristor element predicted theoretically by Chua [9].

Oxygen vacancies acting as charge carriers in memristive devices, they have found growing appreciation in the emerging field of transition-metal oxides responsible for magnetic, orbital, electronic and transport properties.

On the one hand, it is well known that native disorder of perovskite type (ABO_3, *particularly in* $Ba_xSr_{1-x}TiO_3$ *(BST*)) alkaline earth titanates is found to be of Schottky defect type [26-35]. The oxygen vacancies are through to be most mobile and abundant in these perovskite ferroelectrics which may be created or removed by thermal treatment in a reducing or oxidizing atmosphere respectively. They may move and redistribute under the applied external fields [27-30] and form dipoles especially near the electrode/ferroelectric interfaces. In addition, the shift of the charged oxygen vacancies causes local changes in dielectric properties [31-33]. The Auger microprobe dates show [32,33] that oxygen concentration is not constant across the thickness of the film. Near the electrodes it drops to approximately 50% of its value in the center of the film. This creates n-type layers near the electrodes in contrast to the p-type BST regions in the middle of the film [31-33]. It is assumed that the donor state is strongly localized around the nearest titanium ions. In the neutral state the donor level is double occupied, and there is a reduced repulsive interaction between the vacancy and neighboring cations.

At sufficiently high temperatures and/or high fields, the oxygen vacancies are double ionized, acts as donors, each supplying two electrons to the conduction band [26-30]: $O_0 \leftrightarrow \frac{1}{2}O_2(gas) + V_0^{\cdot\cdot} + 2e^-$. An–interstitial oxygen atom may form different types of defects $x = O^0,\ O^-,\ O^{2-}$, which corresponds to three different energies in the energy band. The electrical and optical properties investigations of the deep levels in $SrTiO_3$ thin film show [26-30], that there is a series of deep-level traps with energies in the range of $E_v+2.4eV$ to $E_v+3.15eV$ and a series of shallower traps near the conduction band: $E_c - E_{tn}=0.06 \div 0.4eV$. In the as-grown film the defect concentration is in the range of 10^{14} to 10^{18} cm^3. Higher concentrations (10^{20}-10^{22} cm^3) are also reported [26-28, 34]. The interfacial vacancies cause distortion of the crystal lattice and polarization fields around the vacancy. This makes the levels deeper and causes them to act as charge traps [27-33]. The interfacial built-in electric fields associated with the trapping centers and oxygen vacancies results in changes in the interfacial permittivity of the films [31]. The charge carrier can be trapped by the defects inside the insulator layer or by the electrode/insulator interface, which will build an internal electric field and impact the injection or transport of the carrier that eventually leads to the RS behavior. It can be assumed that the relaxation time is defined by the electron emission process from the trap energy level E_t localized in the energy gap.

As it is indicated above, the inevitable presence of OV in perovskite type ferroelectrics, its migration, as well as the electrons PF ionization mechanisms from OV conditioned trap levels are responsible for a many of switching mechanisms in memristor structures. On the other hand, PF ionization effects in turn contribute to change not only the migration processes of OV, but also to change of electric activities of point defects, its concentrations, energy distribution and particularly its electronic spectra.

The main goal of the present article is the theoretical investigation of OV conditioned trap levels occupation function, f(t), its time dependencies on external electric field, trap levels energy distribution, its characteristic capture and escape times, as well as dependencies on perovskite material other fundamental parameters, which are tied to do for the first time.

In these connections it is interesting (reasonable) to investigate (understand) and discussed the "structure" of switching times of memristors and its connection with the active material and switching mechanism parameters.

We think that under the externally applied electric fields when PF emission becomes dominant the occupation function decreases significantly which leads to creation of new non-compensated charged oxygen vacancies [31]. These charged vacancies under external and internal fields can migrate to the negatively charged electrode and hence "alignment" statistically distributed oxygen vacancies chains.

As for the fully physics-based descriptive and predictive modeling of nonlinear dynamic behavior of memristor, it needs to involve some new internal state variables, for example as it has been done in the case of ferroelectric tunnel junctions (FTJs) [6, 35], with 10 ns operation speeds, where proposed volume fraction of down domains as the state variable. We think, that traps energy distribution, its occupation function time and material parameters dependence can act as an internal state variable function for certain switching structures and mechanisms which are out of frame of the present discussion and is the subject of another investigation.

2. Motivations

One of the most important parameters of the memristive circuits and system is the switching time (the resistance switching time is typically $t_s \leq 10^{-7}$ s) from high-to low impedance [2-17]. The main requirements on memristors are the possible very low programming voltages and switching times [7]. In high-density 1-selector-1 ReRAM arrays real time transient switching (TS) speed responses and delay times also play an important role in operating the memory which are in the range of a few ns [6,35,36]. As it is stated in [36] actual choice of window function is of significant importance for the predictive modelling of memristors when such memristors are driven by periodic alternating polarity pulses. It is observed that the pinched hysteresis loop is a function of excitation frequency and is shrunk by increasing the excitation frequency [9-17]. In fact, as the frequency increases towards infinity, the memristor acts as a linear resistor. In neuromorphic engineering field analog resistive switching of the artificial synapses for adjusting of learning time constant of the spike-timing dependent plasticity (STDP) the trapped electron occupation function shape and dependence on external fields and signal parameters also is important [10-14, 37-38]. Double-barrier devices are interesting candidates for use as artificial synapses in neuromorphic circuits and may pave the way to a real-time implementation of a pattern recognition system. For realistic mathematical description of the device behavior from the obtained experimental data for network-level applications, the memristive biological plasticity model is used [37, 38] and for synaptic plasticity measurements on single devices, rectangular voltage pulses with different amplitudes, polarities, and pulse durations were applied to the devices. For design of autonomous memristor-based oscillator generating periodic signals an external sinusoidal excitation is–needs to be in the autonomous system. This memristor-based oscillator can generate periodic, chaotic, and hyperchaotic signals under the periodic excitation and an appropriate set of circuit parameters [39].

From the above mentioned it is followed that in the *m-f-m* structured memristors where oxygen vacancies creation, migration, the PF emission and trapping/detrapping processes are dominated, as the "lifetime" of trapped electrons usually a few order high than the escape and transit time through to device, during of operation under the different periodic alternating polarity

pulses, the relationship between these times, as well as the trap levels occupation function time dependencies, *f(E,t)*, may play an important role for memristor performance.

3. Model description

Let's consider (*Pt-BST-Pt)* metal-ferroelectric-metal capacitive structure. For evaluation the dependence of the trapped charge carriers concentration, n_t, their occupation function, *f(t)*, (assume that *f(t)* corresponds to Fermi-Dirac distribution) on applied (resulting) field and trapping/detrapping processes due to *PF* mechanism let's assume that the concentration of oxygen vacancy is N_t and that a little amount of free electrons concentration is n_{co} (before applied field).

It is assumed that without an externally applied electric field the vacancy is neutral due to trapped electrons. Under applied external electric field, E_{ext}, when qE_{ext}, exceeds the activation energy, the electrons are detrapped via Poole-Frenkel emission, the vacancy gets charged, and the electric field of the charged vacancy polarizes the crystal predominantly along the applied field locally reducing its permittivity (Fig. 1) [31]. As it is well known [40-42] trapping/detrapping effects in turn are characterizied with the excape, capture times, as well as trap levels occupation function, *f(E,t)*.

For the calculation of trapped electrons concentration, n_t, according to Schottky- Read [40-42] one can get:

$$\frac{\partial n_t}{\partial t} = \sigma v_{th} n_{c0}\left(N_t - n_t\right) - n_t N_c v_{th}\sigma \exp\left(-E_t/kT\right), \qquad \frac{\partial n_t}{\partial t} = r_{cE} - r_{ex},$$

where σ and v_{th} are the capture cross section and the thermal velocity of electrons, respectively, r_{cE} and r_{eE} are the rate of electron capture and release from traps, respectively, N_c is the density of the states in conduction band, E_t is the energy depth of trapped electron, k is the Boltzmann's constant, T is the absolute temperature.

At the thermal equilibrium $\frac{\partial n_t}{\partial t} = 0$, ($r_{cE} = r_{eE}$) one can obtain the concentration of trapped electrons:

$$n_{to} = \frac{N_t n_{co}}{n_{co} + n_1} = \frac{N_t}{1 + n_1/n_{c0}},$$

where n_1 is the Schottky- Read state factor ($n_1 = N_c \exp(-E_t/kT)$ [40-42]).

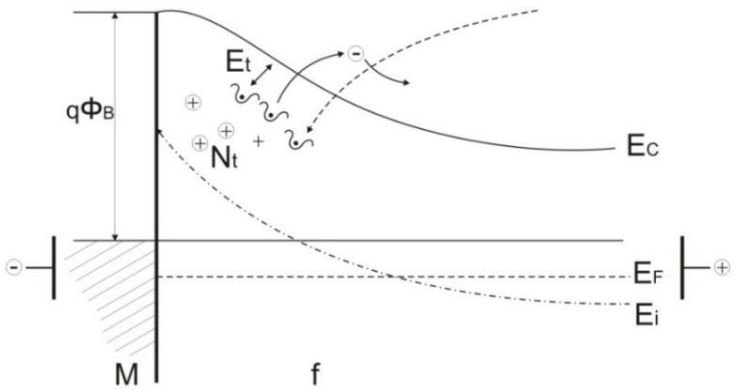

Fig. 1. Schematics of energy band diagram of *m-f* contact under bias (with negative bias of metal-*m*).

If we assume that at the thermal equilibrium (absence of external field) all trap levels are occupied, we obtain $n_{to} \approx N_t$ (as it is known from physics of semiconductors when $|E_t| >> 3kT,\ n_1 << n_{c0}$, $n_{to} \approx N_t$). We assume that when field is applied *PF* release of electrons from the traps (Fig. 1) dominated in comparison with injection from Schottky barrier.

For this condition we obtain

$$\frac{dn_t}{dt} = N_t f(E,t)\vartheta \exp\left(-\frac{qE_t}{kT} + \beta_{PF}\sqrt{E}\right) - n_c N_t\left[1 - f(E,t)\sigma V_{th}\right], \qquad (1)$$

where $f_t(E,t)$ is the field and time dependent electron distribution function (occupancy factor), n_c is the free electron concentration at the presence of the field, ϑ is the "attempt to escape" frequency which is connected to relaxation time with the relationship:

$$\tau_r = \left(\frac{1}{\vartheta}\right)\exp\left[\left(E_t - \Delta\Phi_t\right)\Big/ kT\right],$$

where $\Delta\Phi_t$ is the barrier lower due to *PF* ionization of traps and [40-42], $\Delta\Phi_t = \beta_{pF} kTE_{loc}(x)^{1/2}$, $\beta_{pF} = 2\beta_s$, $\beta_s = \left(\frac{q}{kT}\right)\left(\frac{q}{\pi\varepsilon_{op}(x)}\right)^{1/2}$, β_s - is the Scottky barrier lowering, q– is the electron charge, E_{ext} is the local field distribution in the vicinity of the charged defect [31].

The Poole-Frenkel model, considered below, is based on the hydrogen model where the defect with the bounded (trapped) electron is immersed into a dielectric. In this model the point charge with the bounded electron (i.e., before detrapping) represents an "oscillator" that contributes to the dielectric permittivity in the optical limit, i.e., well above the soft mode. In other words, it is associated with electronic polarization. Thus, in contrast to the microwave permittivity used in the dielectric model above, in the PF model considered below, the permittivity is taken in the optical limit (ε_{op}) and it characterizes only the charge detrapping process, not the dielectric permittivity at microwave frequencies [31].

The capture rate r_{cE} at the presence of the field in the range of energy of E_t $E_t + \Delta E_t$ becomes:

$$r_{cE} = n_c N_t\left(1 - f_t(E)\right)\sigma v_{th} dE_t,$$

and the emission rate:

$$r_{eE} = N_t f_t(E) v \exp(-E_t/kT)\exp\left(\beta_{pF} E^{1/2}(x,t)\right)dE_t.$$

For each equilibrium conditions $r_{cE} = r_{eE}$ and the distribution function, $f_t(E,t)$ becomes:

$$f_{t0} = \left\{1 + \frac{\vartheta \exp(-E_t/kT)\exp\left(\beta_{pF}\sqrt{E_{loc}(x,t)}\right)}{n_c \sigma v_{th}}\right\}^{-1} \qquad (2)$$

If we assume that with the *PF* release of electrons from the traps there takes place injection from the Schottky barrier simultaneously (Fig.1), for $f_t(E,t)$ we obtain:

$$f_n = \left\{1 + \left(\frac{\vartheta \mu_n q}{J_{ns}\sigma V_{tn}}\right)E(x,t)\cdot\exp\left[\beta_{PF}\left(E(x,t)\right)^{\frac{1}{2}}\right]\cdot\exp\left[-\beta_s\left(E(0)\right)^{\frac{1}{2}}\right]\cdot\exp\left(-\frac{E_t}{kT}\right)\right\}^{-1},$$

with $J_{ns} = A^* T^2 e^{-\frac{q\Phi_n}{kT}}$, where *A** is Richardson's constant, Φ_n is the Schottky barrier height, $E(0)$ is the electric field in surface of Schottky barrier.

This case is not considered here. Here we are assuming that without an externally applied electric field the vacancy is neutral due to trapped electrons. Under applied external electric field, the electrons are detrapped via the Poole-Frenkel mechanism and create new charged vacancy. The electric field of the charged vacancy changed the traps level occupation function, $f_t(E,t)$, as well as polarizes the surrounding crystal locally reducing its permittivity [31]. If assume that during of the whole time, when electric field is absence, all traps are occupied and $n_{to} \approx N_t$, for $\frac{n_t(E(x),t)}{n_{to}}$ we obtain:

$$\frac{n_t(E(x),t)}{n_{to}} \approx f_t(E_{loc}(x,t)) .$$

The external field dependent density of the charged vacancies (or, the concentration of non-compensated oxygen vacancies), $n^+{}_t(E_{ext},t)$, we can present as:

$$n_t^{+}(E_{ext},t) = [1 - f_t(E_{ext},t)]N_t \tag{3}$$

As it is evident from (2), with the increase of $E(x,t)$ the $f_t(E,t)$ is decreased.

The decreasing of $f_t(E,t)$ is equivalent to the situation that a certain amount of trapped centers are ionized (released) and the negative charges do not able to neutralize of vacancy conditioned positive charges, which in turn leads to increase of non-compensated vacancies concentration, (charged defects). As a result, in the vicinity of the non compensated defect region will generate $E_{\text{int}}(x,t)$ high field. As it shown by as earlier [31]:

$$E_{loc}(x,t) = E_{\text{int}}(x,t) \pm E_{ext}(x,t),$$

where "+" is taken for the external field which coinsides with the direction of $E_{\text{int}}(x,t)$ and "-" on the oposide sidescases.

Lets, $N_t \sigma V_{th} = \frac{1}{\tau_t}$ - is the electron capture rate, i.e. τ_t - is the time, during which electron is in conductance band, (i.e. "lifetime" of the electrons in conductive band), and $\vartheta \exp\left(-\frac{qW}{kT} + \beta_{PF}\sqrt{E_{loc}(x,t)}\right) = \frac{1}{\tau_p}$ is the rate of electron realize from the trap, i.e. the "lifetime" of electrons in traps. Under these assumptions, the Eq's (1) becomes:

$$\frac{dn_t}{dt} = \frac{N_t f(E,t)}{\tau_p} - \frac{n_c}{\tau_t}[1 - f(E,t)], \quad \frac{dn_t}{dt} = -N_t \frac{df(E,t)}{dt},$$

$$N_t \frac{df(E,t)}{dt} + \frac{N_t f(E,t)}{\tau_p} + \frac{n_c f(E,t)}{\tau_t} - \frac{n_c}{\tau_t} = 0, \quad \frac{df(E,t)}{dt} + \frac{f(E,t)}{\tau_p} + \frac{n_c f(E,t)}{N_t \tau_t} - \frac{n_c}{N_t \tau_t} = 0,$$

$$\frac{df(E,t)}{dt} + f(E,t)\left[\frac{1}{\tau_p} + \frac{\beta_t}{\tau_t}\right] - \frac{\beta_t}{\tau_t} = 0, \tag{4}$$

where $n_1 = \frac{\beta_t}{\tau_t}$, $n_3 = \frac{\tau_t + \beta_t \cdot \tau_p}{\tau_p \cdot \tau_t} = \frac{1}{\tau}$, $\tau = \frac{\tau_t \cdot \tau_p}{\tau_t + \beta_t \cdot \tau_p}$.

The value of the τ can be act as any "specific "(common) time-constant characteristic for the $f_t(E,t)$ distribution.

The solution of Eq.(3) with the boundary conditions: $t = 0$, $E = 0$, $f(0,0) \to f_0$, gives

$$f(E,t)=\left(f_0-\frac{n_1}{n_3}\right)\cdot e^{-n_3 t}+\frac{n_1}{n_3},\quad \frac{n_1}{n_3}=\frac{\beta_t}{\tau_t}\cdot\frac{\tau_p\cdot\tau_t}{(\tau_t+\beta_t\cdot\tau_p)}=\frac{\beta_t\cdot\tau_p}{\tau_t+\beta_t\cdot\tau_r}=\frac{\beta_t\cdot\tau}{\tau_t},$$

$$f(E,t)=\left(f_0-\frac{\beta_t\cdot\tau}{\tau_t}\right)\cdot\exp\left[-\frac{t}{\tau}\right]+\frac{\beta_t\cdot\tau}{\tau_t}\ . \tag{5}$$

For the simplicity let's assume that $t=0$, $E=0$, condition all oxygen vacancies are compensated via traps capture electrons, i.e. $t=0$, $E=0$, $f(E,t)\to 1$ and for $f_t(E,t)$ we obtain:

$$f(E,t)=\left[1-\frac{\beta_t\cdot\tau}{\tau_t}\right]\cdot e^{-\frac{t}{\tau}}+\frac{\beta_t\cdot\tau}{\tau_t}, \tag{6}$$

with

$$\exp\left\{-\frac{qW}{kT}+\beta_{PF}\sqrt{E}\right\}=\frac{N_c\cdot\tau_r}{n_t\cdot\tau_t},\ \text{and}\ \ \vartheta\frac{N_c\cdot\tau_r}{n_t\cdot\tau_t}=\frac{1}{\tau_r},\quad t=\tau\cdot\ln\left[\frac{\left(1-\frac{\beta_t\cdot\tau}{\tau_t}\right)}{\left(f(E,t)-\frac{\beta_t\cdot\tau}{\tau_t}\right)}\right].$$

The occupation function characteristic "time constant" or so-called "relaxation" time corresponds to the condition of $t=\tau$ when $f(E,t)$ decreases in 2,72 time and for $t=0$ $f(E,t)\to 1$ and for $t\to\infty$

$$f(E,\infty)=f_\infty(E,t_\infty)=\frac{\beta_t\cdot\tau}{\tau_t}.$$

The numerical calculations has been carried out according to Eq. (3,4) for the following values of the parameters: $\varepsilon_0=8.85\cdot10^{-14}F/cm$, $\varepsilon_f(0)=300$, $\vartheta\approx10^{12}s^{-1}$, $N_t=(10^{16}\div10^{19})cm^{-3}$, $\sigma=10^{-14}\div10^{-16}cm^2$, $N_c\approx10^{17}cm^{-3}$, $n_c=10^{10}\div10^{13}cm^{-3}$, $E_t=(0.06\div0.4)eV$, which has been taken from the experimentally investigated real structures, carried out in [26-35,43]. The results of theoretical calculations of *m-BST-m* structures are presented in Fig. 2 - Fig. 6.

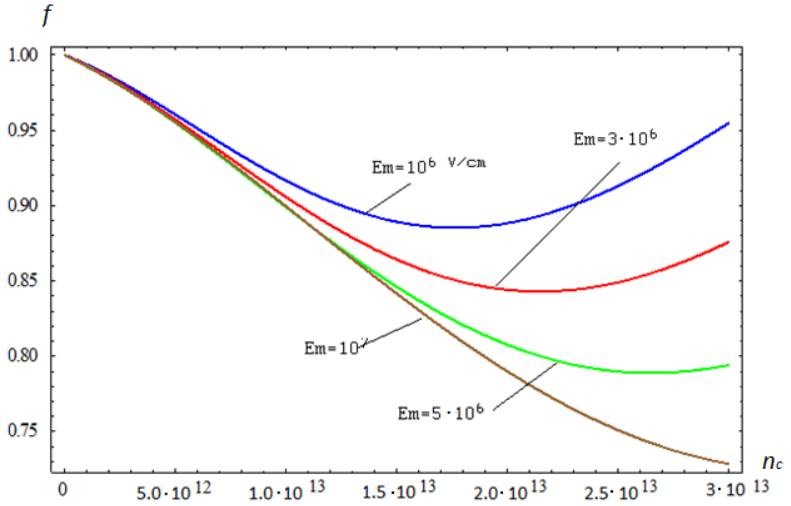

Fig. 2. Dependence of distribution function $f(E,t)$ on free electron concentration $n_c(cm^{-3})$ for the different values of electric field $E_m(V\cdot cm^{-1})$, ($N_t=10^{18}cm^{-3}$; $\tau_t=10^{-8}s$; $\tau_p=0.005s$; $\varepsilon_f=300$; $t=0.05\cdot10^{-5}s$, $v_{th}=10^7cm\cdot s^{-1}$, $E_t=0.36eV$, $\vartheta=10^{12}s^{-1}$, $\sigma=10^{-14}cm^{-2}$).

a)

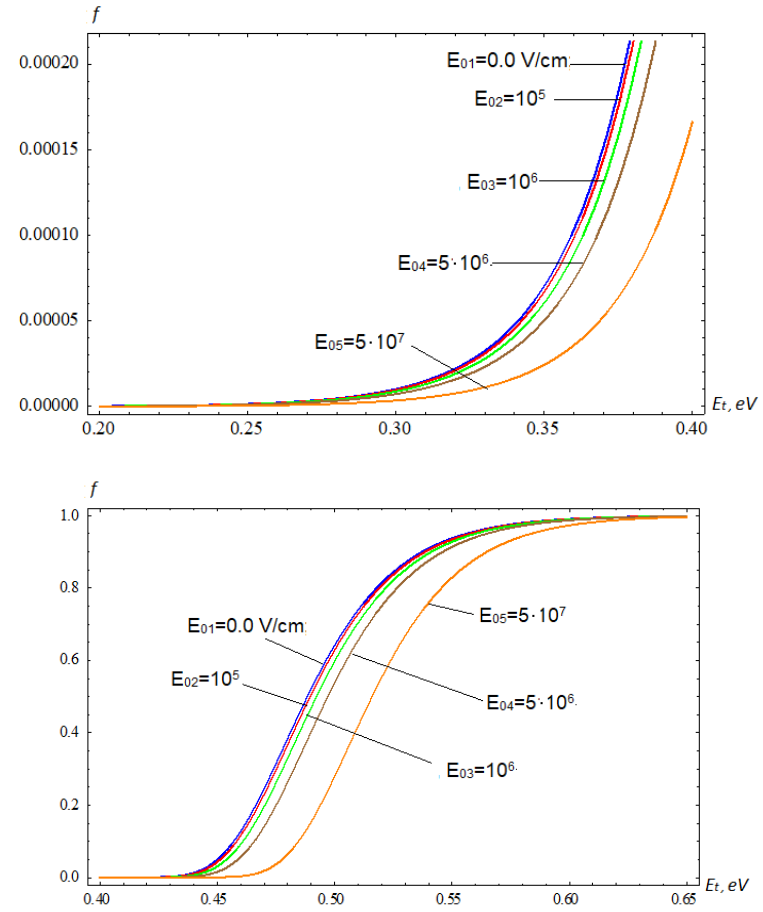

Fig. 3. a, b) Dependen b) istribution function $f(E,t)$ on energy depth of traps $E_t(eV)$ for different value of applied field $E_0\left(V\cdot cm^{-1}\right)$ ($t=0.05\cdot10^{-5}s$, $N_t=10^{18}cm^{-3}$; $\tau_t=10^{-8}s$; $\tau_p=0.005s$; $\varepsilon_f=300$, the other parameters as in Fig. 2).

a) b)

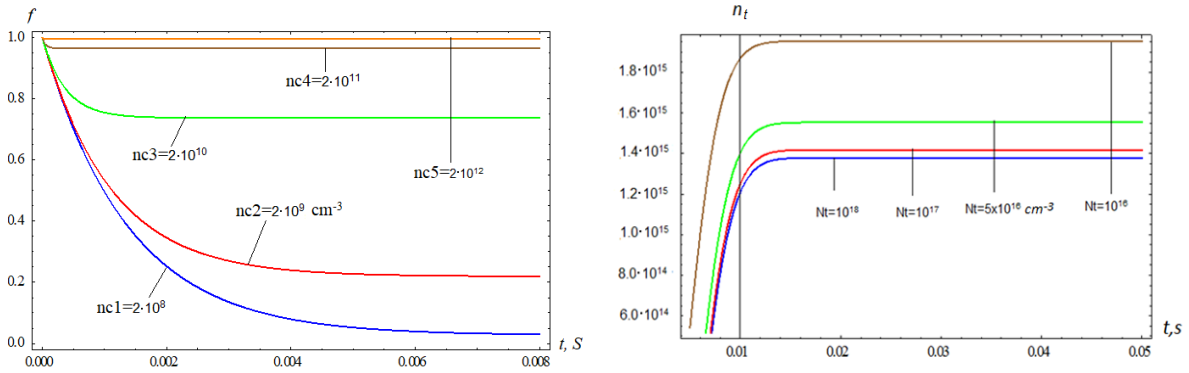

Fig. 4. a) Dependence of traps distribution function $f(E,t)$ on time ($tx10^{-4}\,s$) for different values of free electron concentration $n_c\,(cm^{-3})$. b) Dependence of density of charged vacancies $n^{+}{}_{t}(cm^{-3})$ on time t for different values of $N_t(cm^{-3})$, ($n_c = 10^{12} cm^{-3}$, $E_0 = 7\cdot 10^6$ Vcm^{-1}, $E_t \equiv 0.56.(eV)$, the other parameters as in Fig. 2).

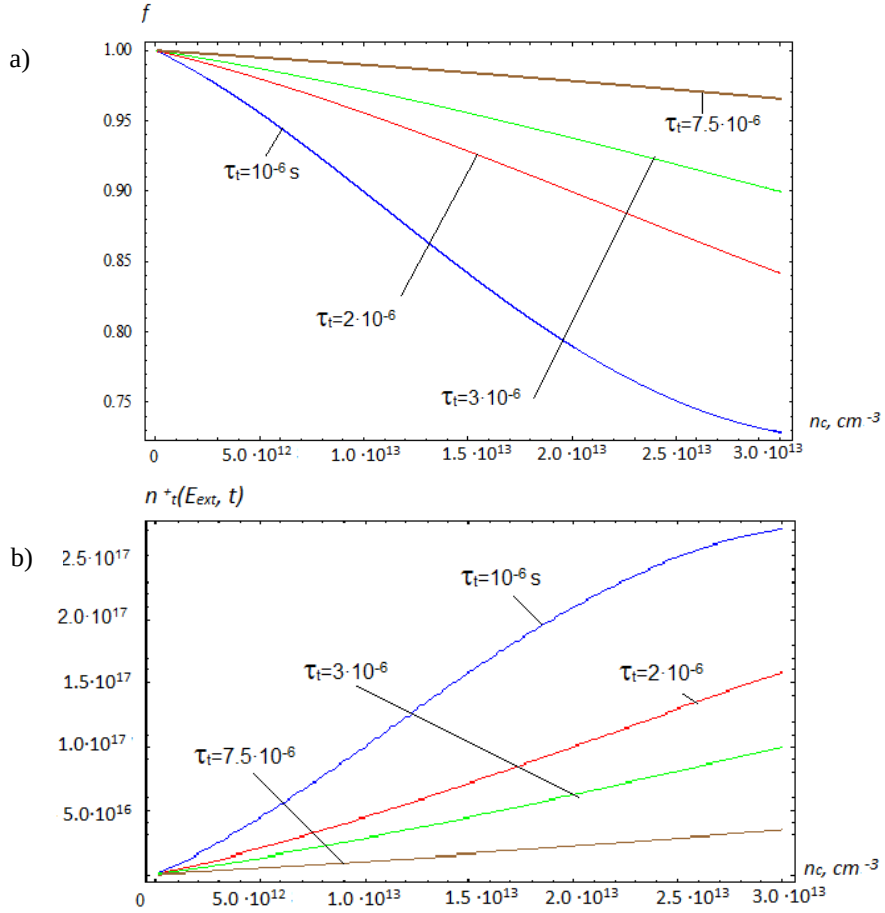

Fig. 5. Dependence of traps distribution function *f(E,t)* (a) and dependence of charged vacancies concentration $n^{+}{}_{t}(cm^{-3})$ (b) on free electron concentration $n_c(cm^{-3})$ for the different values of parameter τ_t (the other parameters as in Fig. 2 and Fig. 3).

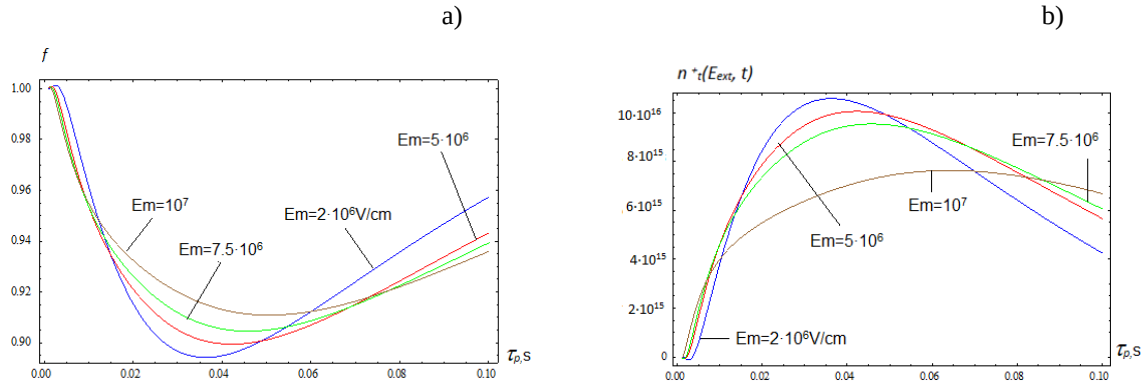

Fig. 6. Dependence of traps distribution function *f(E,t)* (a) and dependence of charged vacancies concentration $n^{+}{}_{t}(cm^{-3})$ (b) on parameter τ_p for different values of applied field $E_m(V\cdot cm^{-1})$

(the other parameters as in Fig. 2 and Fig. 3).

4. Conclusions

As it is expected, the changes of occupancy probability, $f(E,t)$, and hence, the change of concentration of charged oxygen vacancies, $n_t^+(E,t)$, under the influence of applied electric field, one can be associated with the Poole-Frenkel emission of captured electrons from oxygen vacancies conditioned trap levels. As it is followed from expressions (3-6), with the increase of the electric field, as well as with the increase of the concentration of free electrons, $f(E,t)$ and therefore $n_t^+(E,t)$ will decrease (Fig. 2, Fig. 5). As deeper the energy depth of trap levels, E_t , the occupation function is high and as high the electric field a long time is required for change of the $f(E,t)$ and $n_t^+(E,t)$ (Fig. 3, Fig. 6). As higher N_t (concentration of oxygen vacancies) and smaller of free electron concentration, n_c, the density of the charged vacancies, $n_t^+(E,t)$, is high.

As it is followed from Fig. 2, Fig. 6 $f(E,t)=g(t,\tau_p)$dependence passed through via minimum which can be explained by this model: for constant concentration of oxygen vacancies, N_t, i.e. trap centers with the increase of its energy dept, E_t , current is decreased due to dominate of capture rate of injected charge carriers in respect of escape from these traps and for the higher energy depth when all traps are occupied (fulled) the escape is becomes dominant in respect of the capture. As high the electric field, the occupation function's decrease takes place very rapidly.

Increase of the τ_t (i.e. lifetime of electrons in conductive band) keeping σV_{th} constant, it means decrease of concentration of oxygen vacancies, N_t, and decrease of $f(E,t)$ (Fig. 6).

These results will contribute to a better understanding of electro-physical and switching processes which take place in m-f-m nano-film based memristors.

We anticipate that the new knowledge that emerges from this study will provide the basis for the development of new idea according which trap levels occupation function, $f_t(E,t)$, can act as an internal state variable for a design and modeling of a new classes memristors where PF current mechanism is dominated as well as to explain the experimental results in these fields more precisely.

Acknowledgments

This work was supported by RA MESCS Science Committee, in the frames of the research project № 19YR-2J050.

References

[1] K. Dimmler, M. Parris, D. Butler et al., J. Appl. Phys. **61** (1987) 12.
[2] D.J Kim, H. Lu, S. Ryu et al., Nano Lett. **12** (2012) 569.
[3] D. Pantel, M. Alexe, Phys. Rev. B **82** (2012) 134105.
[4] A. Chanthbouala, V. Garcia, R.O. Cherifi, et al., Nature Materials **11** (2012) 860.
[5] W. Li, M. Alexe, Appl. Phys. Lett. **91** (2007) 26093.
[6] A. Chanthbouala, A. Crassous, V. Garcia, et al., Nature Nanotech. **7** (2012) 101.
[7] A. Quindeau, D. Hesse, M. Alexe, Front. Phys. **2** (2014) 7.
[8] W. Shen, R. Dittmann, U. Breuer, R. Waser, Applied Physics Letters, **93** (2008) 222102.
[9] L.O. Chua, S.M. Kang, Proc. IEEE **64** (1976) 209.
[10] Y.V. Pershin, M.Di Ventra, IEEE Trans. Circuits Syst. I **57** (2010) 1857Y1864.

[11] Y. V. Pershin, M. Di Ventra, IEEE Circuits and Systems Magazine **12** (2012) 64.
[12] D. Strukov, G. Snider, D. Stewart, R.S. Williams, Nature **453** (2008) 80.
[13] D. Strukov, R.S. Williams, Applied Physics A: Materials Science & Processing **94** (2008) 515.
[14] D. Strukov, J. Borghetti, R.S. Williams, Small **5** (2009) 1058.
[15] G. Oster, IEEE Trans. On Circuits and Systems, **21** (1974) 152.
[16] LR. Waser, M. Aono, Nature Materials **6** (2007) 833.
[17] R. Waser, R. Dittmann, G. Staikov, K. Szot, Advanced Materials **21** (2009) 2632.
[18] R.G. Cope, A.W. Penn, Journal of Physics D: Applied Physics **1** (1968) 161.
[19] H.T. Kim, B.J. Kim, S. Choi, B.G. Chae, Y.W. Lee, T. Driscoll, M.M. Qazilbash, D.N. Basov, Journal of Applied Physics **107** (2010) 023702.
[20] F.A. Chudnovskii, L.L. Odynets, A.L. Pergament, G.B. Stefanovich, Journal of Solid State Chemistry **122** (1996) 95.
[21] T. Harada, I. Ohkubo, K. Tsubouchi at al. Appl. Phys. Lett. **92**, (2008) 222113.
[22] S. Hirose, A. Nakayama, H. Niimi, K. Kageyama, H. Takagi, Journal of Applied Physics **104** (2008) 053712.
[23] B. Phan, J. Lee, Applied Physics Letters **93** (2008) 222906.
[24] M. Hasan, R. Dong, H.J. Choi, D. S. Lee, D. J. Seong, M.B. Pyun, H. Hwang, Applied Physics Letters **92** (2008) 202102.
[25] C.H. Yang, J. Seidel, S.Y. Kim, P.B. Rossen, P. Yu, M. Gajek, Y.H. Chu, L.W. Martin, M.B. Holcomb, Q. He, P. Maksymovych, N. Balke, S.V. Kalinin, A.P. Baddorf, S.R. Basu, M.L. Scullin, R. Ramesh, Nature Materials **8** (2009) 485.
[26] H.-M. Chen, V; Y.-P. Wang, T.-J. Tseng., J. Appl. Phys. **81** (1997) 6762.
[27] G.W. Dietz, W. Antipohler, M. Klee et al., J. Appl. Phys.**78** (1995) 6113.
[28] W. A. Feil, B. W. Wessels, Journal of Applied Physics **74**, (1993) 3927.
[29] R. Meyer, R. Liedtke, R. Waser, Applied Physics Letters **86** (2005) 112904.
[30] J. Robertson, J. of Applied Physics **93** (2003) 1054.
[31] V. Buniatyan, N. Martirosyan, A. Vorobiev et al., J. of Applied Physics **110** (2011) 094110.
[31] J. Antula, J. Appl. Phys. **94** (1972) 4663.
[32] M. Dawber, J.F. Raba, J.F. Scott, Rev. of Modern Phys. **77** (2005) 1083.
[33] J. Gerblinger, H. Meixner, J. of Applied Physics **67** (1990) 7453.
[34] C.H. Park, D.J. Chadi, Phys. Rev. B **57** (1998) 13961.
[35] Y. Shang, W. Fei, H. Yu., IEEE transactions on circuits and systems I **59** (2012) 1906.
[36] V.A. Slipko, Yu.V. Pershin, Preprint arXiv:1811.06649 (2018).
[37] M. Ziegler, C. Riggert, M. Hansen, T. Bartsch, H. Kohlstedt, IEEE Trans. Biomed. Circ. Syst. **9** (2015) 197.
[38] S. Dirkmann, M. Hansen, M. Ziegler, H. Kohlstedt, T. Mussenbrock, Scientific Reports **6**, (2016) 35686.
[39] G. Wang, M. Cui, B. Cai, et al. Mathematical Problems in Engineering **2015** (2015) 561901.
[40] S. M. Sze, Physics of Semiconductor Devices (Second Ed. J. Wiley & Sons. 1981).
[41] M. A. Lampert, P. Mark, Current Injection in Solids (Acad. Press New-York and London 1970).
[42] A.G. Milnes, Deep Impurities in Semiconductors (John Wiley & Sons, New-York, 1977).
[43] V. Buniatyan, V. Begoyan, A. Davtyan et al., Advanced Materials & Technologies No. 1, (2019) 35.